THE FATIGUE CRACK DIRECTION AND THRESHOLD BEHAVOUR OF A MEDIUM STRENGTH STRUCTURAL STEEL UNDER MIXED MODE I AND III LOADING

L P Pook and D G Crawford
National Engineering Laboratory
East Kilbride, Glasgow G75 OQU, Scotland

Third International Conference on Biaxial/Multiaxial Fatigue
April 3-6 1989, Stuttgart, FRG

ABSTRACT

As part of a programme to investigate mixed mode fatigue crack growth threshold behaviour, tests were carried out on a medium strength structural steel to BS 4360 Grade 50D. The three-point bend specimens used had spark eroded initial slits inclined to give mixed Mode I and III displacements. Baseline Mode I tests were also carried out. Crack growth was monitored by alternating current potential drop equipment.

Overall, the expected tendency to Mode I crack growth showed as an initial discontinuity followed by a smooth rotation of the crack front towards a direction perpendicular to the specimen sides. At a smaller scale, initial crack growth was by the formation of Mode I facets which developed into a 'twist' fracture surface consisting of narrow Mode I facets interlinked by cliffs, the facets tending to merge as a crack grew.

The experimental mixed Mode I and III fatigue crack growth threshold data were close to a lower bound failure envelope based on the premise that the event controlling failure is the propagation of Mode I branch cracks. Experimental fatigue crack growth rates for propagating twist fractures were less than would be anticipated on the basis of their apparent Mode I stress intensity factor ranges. Estimated stress intensity factor corrections for twist fractures based on facet overlap led to a satisfactory lower bound to the experimental data.

1 INTRODUCTION

As part of a programme [1] to investigate mixed mode fatigue crack growth threshold behaviour, tests were carried out on a medium strength structural steel to BS 4360 Grade 50D. The three point bend specimens used had spark eroded initial slits inclined to give mixed Mode I and III displacements. Baseline Mode I tests were also carried out. Crack growth was monitored by alternating current potential drop (ACPD) equipment. Tests using similar specimens have previously been carried out to determine the crack direction and threshold behaviour of mild steel [2].

The present tests had three main aims. Firstly, to see whether the pattern of crack growth was the same as that previously observed [2] in mild steel. Secondly, to determine the fatigue crack growth threshold of relatively long cracks for mixed Mode I and III loading and compare the results with data for other steels, and finally to collect fatigue crack growth rate data in the near threshold region. Relevant theoretical and specimen design considerations are discussed in References 1 and 2.

As fatigue crack growth is normally in Mode I, crack growth data can be conveniently analysed in terms of the Mode I stress intensity factor, K_I. The range of K_I in the fatigue cycle, ΔK_I, is usually the major variable. A threshold value of ΔK_I, ΔK_{th}, must be exceeded before a crack will grow. The prefix Δ indicates range in the fatigue cycle; in this paper it is sometimes omitted. The mixed Mode threshold data are given in terms of K_I, K_{III}, which is the Mode III stress intensity factor, and K_A, which is the apparent Mode I stress intensity factor. The crack growth data are given in terms of K_A.

2 TEST METHOD

The pedigree material [3] used was a structural steel to British Standard 4360 Grade 50D. The average values of the tensile strength and the 0.2 per cent proof stress were 513 and 370 MN/m² respectively. The grain size, measured by the intercept method, was 10 μm.

Three point bend specimens, of the design shown in Fig. 1, were cut from a single plate with their length and thickness dimensions in the longitudinal and short transverse directions respectively. The expected crack path for

this type of specimen [2] is shown schematically in Fig. 2. A spark eroded slit was used to avoid difficulties associated with precracking mixed mode specimens in fatigue; its use has previously been found satisfactory for mild steel [2].

All tests were conducted in air at room temperature (average 21°C) using a test frequency of 100 Hz, a support span of 240 mm and an R value (ratio of minimum to maximum load in the fatigue cycle) of 0.1. In most cases the loads applied were increased incrementally using a specially written program. β values (Fig. 1) of 90°, 75°, and 60° were used, giving pure Mode I and K_{III}/K_I ratios of 0.27 and 0.58 respectively. Test conditions for individual mixed mode specimens are summarised in Tables 1 and 2. The numbers of cycles at each load level, and within each load level the numbers of increments over which crack growth was measured, are included.

Crack length was measured using an alternating current potential drop (ACPD) system. The particular system used had a resolution of 0.01 mm, a short-term accuracy of 0.02 mm and a temperature sensitivity of about 0.04 mm/°C. Because of the high test frequency, sampling the ACPD signal at the maximum load in the cycle was impractical so the readings obtained provided an average over the whole fatigue cycle. The calibration was checked initially by using crack front markings due to load changes on $\beta = 90°$ specimens. For $\beta = 75°$ and 60° calibration was based on the measured crack length at the end of a test. Minor temperature changes resulted in drift in the ACPD equipment and led to some difficulties in interpreting results. There were some instances of apparently negative increments of crack growth, the resulting apparently negative crack growth rates being taken as zero.

A variety of techniques can be used to determine fatigue crack growth thresholds [1, 4]; the method chosen here was to calculate the threshold from the highest load increment at which the crack growth rate did not exceed 2×10^{-8} mm/cycle. The threshold data are shown to three significant figures; the accuracy of the data do not justify the third figure but it is included to avoid excessive rounding errors. Near threshold fatigue crack growth rates were calculated using the second method. Equations used in calculations are given in the Appendix. The ratio of nominal net section stress to the 0.2 per cent proof stress was approximately 0.2 for the threshold data, and did not exceed 0.4 for the fatigue crack growth rate data. After testing, specimens were broken open at low temperature so that the fracture surfaces could

be examined. In the mixed mode specimens testing was discontinued after between 3 and 10 mm of crack growth.

3 RESULTS

Baseline Mode I fatigue crack growth thresholds obtained from specimens MGLA 1, 2 and 3 were 7.38, 6.82 and 7.46 $MN/m^{3/2}$ respectively, giving a mean value of 7.2 $MN/m^{3/2}$. This is typical for a fine grained alloy steel [4]. The corresponding plastic zone size, r_p, calculated from the maximum load in the fatigue cycle using Equation (5), was 0.025 mm. Because of the use of $\beta = 90°$ specimens to calibrate the ACPD equipment, relatively few baseline fatigue crack growth rate data were obtained (Fig. 3a). However, they agree well with published data for similar steels [4], and appear to be reliable.

The mixed Mode I and III fatigue crack growth thresholds obtained are given in Table 3. K_A is the apparent value of K_I calculated using equation (1) as if β were 90°; K_I and K_{III} were then calculated using equations (2) and (3). The fatigue crack growth rate data from the mixed Mode I and III specimens are shown in Fig. 3 plotted against ΔK_A in a manner analogous to that conventionally used for pure Mode I data. The data from specimen MGLA 4 (Fig. 3b) extended to very low crack growth rates but this may have been an artefact of drift in the ACPD system. For specimens MGLA 6 ($\beta = 75°$, Fig. 3b) and MGLA 8 ($\beta = 60°$, Fig. 3c), crack growth rates first decreased and then increased, as sometimes observed in 'short crack' tests [5]. Again, this may have been an artefact of drift in the ACPD system, but current tests for $\beta = 45°$ suggest that it is genuine.

The fatigue fracture surfaces of the mixed mode specimens are shown in Figs 4 and 5. With the exception of specimen MGLA 6 (Fig. 4c), crack fronts remained reasonably straight and perpendicular to the expected direction of crack growth. The general appearance of the fracture surfaces was the same as for the mild steel tests [2]. Macroscopically, as a crack grew the crack front rotated towards the $\beta = 90°$ plane; average values of the initial crack growth angle, α (Fig. 2), at the specimen surface are 24.3° and 28.5° for $\beta = 75°$ and 60° respectively.

On a finer scale, initial crack growth was by the creation of small branch cracks which formed a 'twist' fracture surface [2], consisting of what appeared to be narrow Mode I facets interlinked by cliffs, and having the

general appearance of a staircase. In general, the facets extended under the cliffs, suggesting that the latter form as a consequence of facet propagation. The facets then merged with one another as a crack grew. At the start of crack growth the facets were too small and too damaged by fretting for their angles to be measured to confirm that they were indeed Mode I. However, previous work on mild steel [2], where the facets were generally larger, strongly suggests that this was the case. There was clear evidence of crack arrest after several millimetres of crack growth in specimens MGLA 6, 7, 8, and 9 (Figs 4 and 5), suggesting that the crack was not growing along the whole of the (irregular) crack front.

4 DISCUSSION

In interpreting the ACPD data it was assumed that the cracks were sufficiently uniform through the thickness of a specimen to be regarded as 'one-dimensional' [6, 7]. Using this assumption leads to possible errors from three main sources, all of which are unfortunately difficult to quantify, but should have been minimised by the calibration procedure adopted. Firstly, differences in crack length through the specimen thickness; it cannot be assumed that the measured length will be an arithmetic average [6]. Where $\beta = 75°$ or $60°$ the true crack length at the surface is greater than on the specimen centre line, even for a straight crack front. Secondly, point or line contact between opposite faces of a fracture; this short-circuits the current and reduces the apparent crack length. Cliffs between Mode I facets act as line contacts, and can result in significant underestimation of crack length [7]. Finally, overlapping facets increase the current path length leading to overestimates of crack length [8].

Equations (2) and (3) used to calculate values of K_I and K_{III} for the initial slit are only exact for the case of a tunnel crack in an infinite body, but appear to be reasonably accurate near the specimen centre line [2]. Assuming that once crack growth starts the crack is pure Mode I, then the strain energy release rate argument given in the Appendix leads to the conclusion that K_A is actually a reasonable estimate for K_I provided that β is not too small (maximum error 7.5 per cent in K_I at $\beta = 60°$).

Away from the specimen centre line Mode II displacements are present prior to crack growth. This accounts for the abrupt change of crack direction when

crack growth starts, which is such that the Mode II stress intensity factor, K_{II}, is reduced to zero [2]. The initial K_{II}/K_I ratio is largest at the specimen surface where it may be estimated from the initial crack growth angle, α (Fig. 2), using equation (6). For $\beta = 75°$ and 60° the K_{II}/K_I ratios so calculated were 0.23 and 0.25 respectively.

Fig. 6 shows the experimental mixed Mode I and III threshold results normalised using a ΔK_{th} value of 7.2 $MN/m^{3/2}$. They are compared with a lower bound failure envelope based on Mode I branch crack growth and an upper bound failure envelope based on K_I for the initial crack. These bounds proved satisfactory both for the previous tests on mild steel [2] and for tests on a range of steels using circumferentially notched round specimens [9]. Both these data sets are included on the figure. Two points are shown for the mild steel tests at $\beta = 75°$, the one marked 'fine facets' was based on tests where specimens had initial facets comparable in size to those observed on the present test specimens. The results agree well with the earlier data and help to confirm the previous observation [1, 2] that Mode III displacements encourage Mode I branch crack formation, leading to test results which are close to the lower bound. For completeness an envelope based on constant K_A (Appendix) is included on Fig. 6.

The Mode I facets on a twist fracture surface overlap. Stress intensity factors for overlapping cracks are less than those for single cracks. Examination of stress intensity factors both for two closely spaced overlapping cracks and for cracks with two small symmetrical branches at a tip [10] suggests that the stress intensity factor for two overlapping facets is about 3/4 of that for a single facet, and provides an approximate lower bound for the stress intensity factor for a twist fracture surface, assuming that it is unusual for more than two facets to overlap. The fatigue crack growth rate data appear to confirm this lower bound (Fig. 3d); the data for $\beta = 75°$ and 60° fall between those for $\beta = 90°$ and a predicted lower bound (dashed line) obtained by dividing ΔK_A values by 3/4. A similar retardation is sometimes observed in tests on welded joints where overlapping facets occur because of crack initiation at different levels along a weld [7].

5 CONCLUSIONS

The fracture surfaces of the mixed Mode I and III test specimens showed that initial crack growth was by the formation of small Mode I branch cracks which developed into a 'twist' fracture. This consisted of narrow Mode I facets

interlinked by cliffs, the facets tending to merge as a crack grew. Macroscopically, there was an initial directional discontinuity, followed by a smooth rotation of the crack front towards the expected Mode I crack growth plane.

The experimental mixed Mode I and III fatigue crack growth threshold data were close to a lower bound failure envelope based on the premise that the event controlling failure is the propagation of Mode I branch cracks.

Experimental fatigue crack growth rates for propagating twist fractures were less than would be anticipated on the basis of their apparent Mode I stress intensity factor ranges. Estimated stress intensity factor corrections for twist fractures, based on facet overlap, led to a satisfactory lower bound to the experimental data.

ACKNOWLEDGEMENTS

This paper is published by permission of the Director, National Engineering Laboratory, UK Department of Trade and Industry.

REFERENCES

1 POOK L. P. The significant of Mode I branch cracks for mixed mode fatigue crack growth threshold behaviour. BROWN M. W. and MILLER K. J. (Ed). Biaxial and multiaxial fatigue. EGF 3. London: Mechanical Engineering Publications Ltd. 1988, pp 247-263.

2 POOK L. P. The fatigue crack direction and threshold behaviour of mild steel under mixed Mode I and III loading. Int. J. Fatigue, 1985, 7(1), 21-30.

3 ANON. United Kingdom Offshore Steels Research Project - Phase II final summary report. London: HMSO, 1987.

4 TAYLOR D. A compendium of fatigue thresholds and growth rates. Warley, West Midlands: Engineering Materials Advisory Services Ltd, 1985.

5 KENDALL J. M. and KING J. E. Short crack growth behaviour: data analysis effects. Int. J. Fatigue, 1988, 10(3), 163-170.

6 CONNOLLY M. P. and COLLINS R. The measurement and analysis of semi-elliptical surface fatigue crack growth. Eng. fract. Mech., 1987, 26(6), 897-911.

7 CONNOLLY M. P. and DOVER W. D. The measurement and analysis of fatigue crack growth in tubular welded Y and K joints. Proc. Int. Conf. Fatigue of Engineering Materials and Structures, Sheffield, 15-19 September 1986, Proc. I.Mech.E. 1986, Vol 1, pp 129-136.

8 HAQ R, MICHAEL D. H. and COLLINS R. The detection and measurement of overlapping fatigue cracks at welded joints by thin-skin electromagnetic fields. Proc. Roy. Soc. A., 419, pp 69-89.

9 POOK L. P. Mixed Mode I and III fatigue-crack growth thresholds for a range of steels. NEL Report No 703. East Kilbride, Glasgow: National Engineering Laboratory, 1986.

10 MURAKAMI Y. (Ed). Stress intensity factors handbook. Oxford: Pergamon Press, 1987, pp 114, 379, 384, 386.

11 PARIS P. C. and SIH G. C. The stress analysis of cracks. In fracture toughness testing and its applications. ASTM STP 381. Philadelphia, PA: American Society for Testing and Materials, 1965, pp 30-83.

A P P E N D I X

EQUATIONS USED IN CALCULATIONS

For pure Mode I ($\beta = 90°$, Fig. 1) tests values of the Mode I stress intensity factor K_I were calculated using the expression [2]:

$$\frac{K_I B W^{1/2}}{P} = \frac{3(S/W)\alpha^{1/2}\left\{1.99 - \alpha\,(1-\alpha)\,(2.15 - 3.93\alpha + 2.7\alpha^2)\right\}}{2(1+2\alpha)(1-\alpha)^{3/2}} \qquad (1)$$

$$0 \leq \alpha = a/W \leq 1$$

where B is specimen thickness, W is specimen width, P is applied load and S is support span. For $\beta \neq 90°$, apparent values of K_I (K_A) were first calculated using equation (1), and K_I and the Mode III stress intensity factor, K_{III}, were then calculated using the approximate expression [2]:

$$K_I = K_A \sin^2\beta \qquad (2)$$

$$K_{III} = K_A \sin\beta \cos\beta. \qquad (3)$$

For a uniaxial stress field this is equivalent to taking:

$$K_A = K_I + K_{III}^2/K_I. \qquad (4)$$

Values of the plastic zone size at the crack tip, r_p, were estimated for the maximum load in the fatigue cycle using the expression [13]:

$$r_p = \frac{K_I^2(1-2\upsilon) + 3K_{III}^2}{2\pi\sigma_Y^2} \qquad (5)$$

where σ_Y is the 0.2 per cent proof stress and υ is Poisson's ratio, taken as 1/3. The approximate initial crack growth angle, α (Fig. 2) is given by [2]:

$$K_I \sin\alpha = K_{II}(3\cos\alpha - 1) \qquad (6)$$

The strain energy release rate, G, of a Mode I crack, under plane strain conditions, is given by [11]:

$$G = K_I (1 - \nu^2)/E \qquad (7)$$

where E is Young's modulus. Now for a crack at angle β (Fig. 2) the crack front length is $B/\sin\beta$. Hence, if it be assumed that the global strain energy release is independent of β and also that a growing crack is actually in Mode I, it follows that:

$$K_I = K_A (\sin\beta)^{1/2} \qquad (8)$$

which implies that K_A provides a reasonable estimate for K_I provided that β is not too small: $(\sin\beta)^{1/2} = 1$, 0.983, 0.931 and 0.841 for $\beta = 90°$, 75°, 60° and 45° respectively.

T A B L E 1

TEST CONDITIONS, $\beta = 75°$

Specimen number	Width W (mm)	Thick-ness B (mm)	Initial crack length a (mm)	Mean load (kN)	Alt. load (kN)	No of cycles (millions)	No of incre-ments
MGLA 4	60.32	20.14	19.93	2.20	1.80	9.999	1
			20.08	2.44	2.00	10.00	1
			20.03	2.68	2.20	10.00	1
			20.10	2.94	2.40	10.00	1
			20.14	3.18	2.60	10.00	1
			20.33	3.42	2.80	10.00	1
			20.98	3.66	3.00	10.00	1
			23.13*				
MGLA 5	60.27	20.15	19.93	2.90	2.38	158.7	13
			20.32	3.04	2.50	100.0	9
			20.22	3.20	2.62	112.1	7
			20.14	3.36	2.76	102.7	9
			20.38	3.52	2.90	112.4	10
			20.42	4.22	3.48	2.712	8
			26.91*				
MGLA 6	60.26	20.04	19.83	3.72	3.06	21.82	34
			26.53*				

*Final crack length.

T A B L E 2

TEST CONDITIONS, $\beta = 60°$

Specimen number	Width W (mm)	Thick-ness B (mm)	Initial crack length a (mm)	Mean load (kN)	Alt. load (kN)	No of cycles (millions)	No of incre-ments
MGLA 7	60.30	20.20	20.16	2.70	2.25	100.0	20
			20.34	3.24	2.68	100.0	20
			20.03	3.90	3.22	20.13	16
			29.46*				
MGLA 8	60.30	20.18	19.96	3.60	2.95	35.27	49
			29.36*				
MGLA 9	60.31	20.01	19.93	3.40	2.81	99.97	20
			20.09	3.60	2.95	100.0	27
			20.55	3.78	3.11	15.46	20
			29.93*				

*Final crack length.

T A B L E 3

MIXED MODE I AND III FATIGUE CRACK GROWTH THRESHOLDS

Specimen number	β (deg)	ΔK_A ($MN/m^{3/2}$)	ΔK_I ($MN/m^{3/2}$)	ΔK_{III} ($MN/m^{3/2}$)	r_p (mm)
MGLA 4	75	6.95	6.48	1.74	0.034
MGLA 5	75	7.79	7.27	1.95	0.043
MGLA 7	60	7.13	5.35	3.08	0.056
MGLA 9	60	7.95	5.96	3.44	0.070

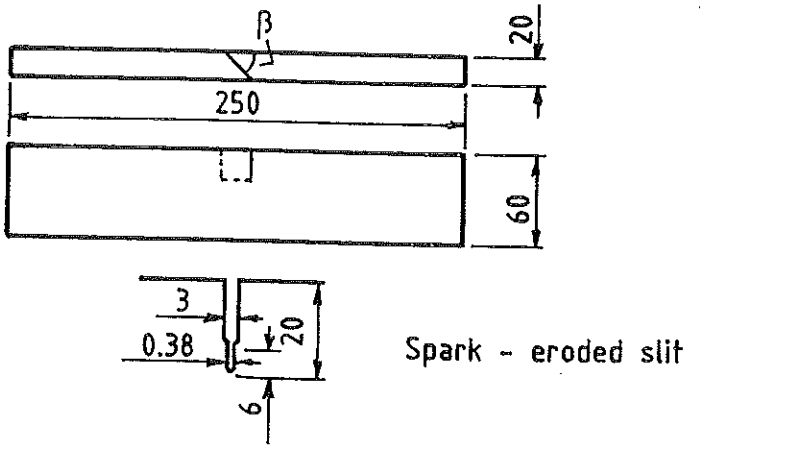

FIG. 1 MIXED MODE I AND III TEST SPECIMEN

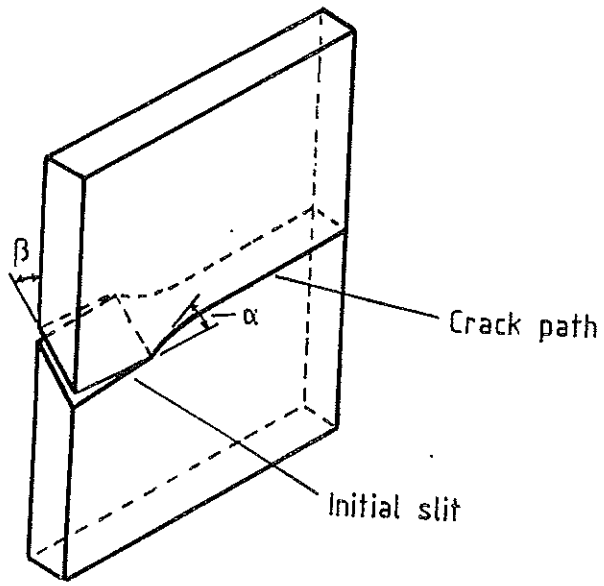

FIG. 2 SCHEMATIC CRACK PATH

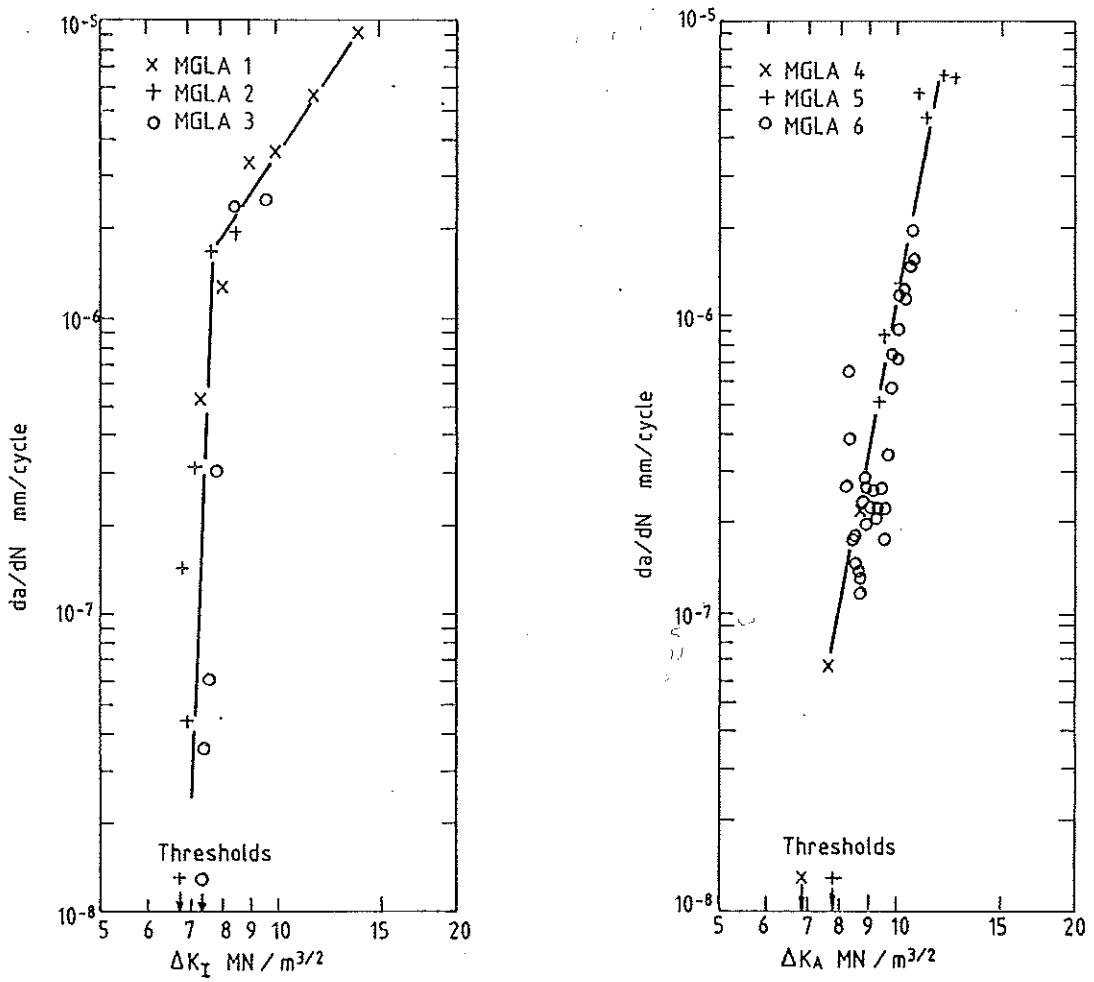

(a) $\beta = 90°$ (b) $\beta = 75°$

FIG. 3 FATIGUE CRACK GROWTH RATE DATA

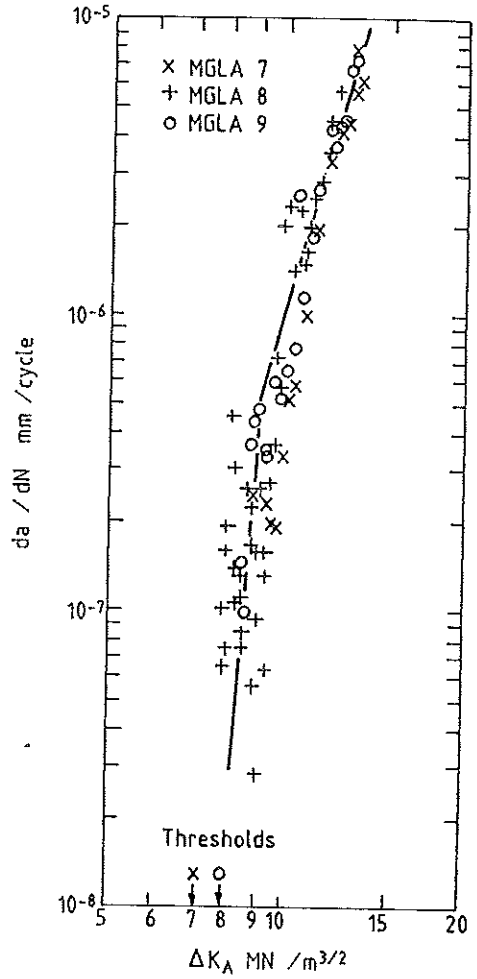

(c) $\beta = 60°$

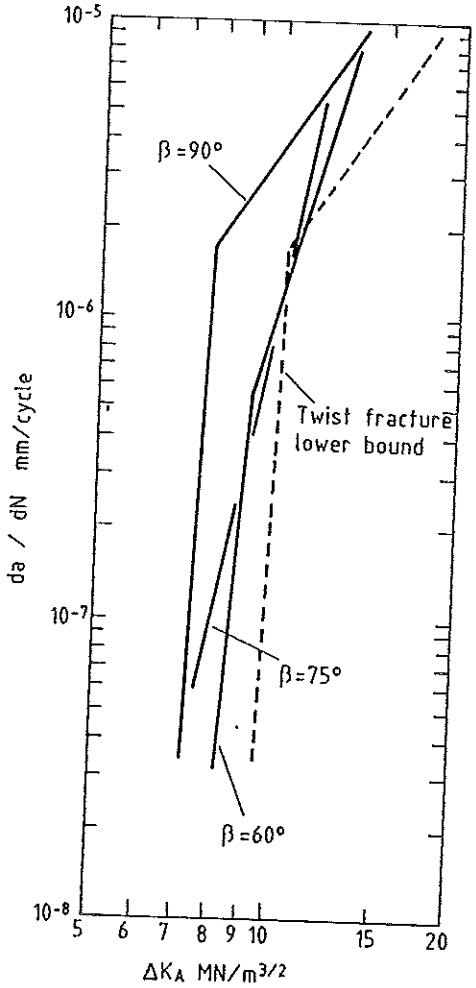

(d)

FIG. 3 (Contd) FATIGUE CRACK GROWTH RATE DATA

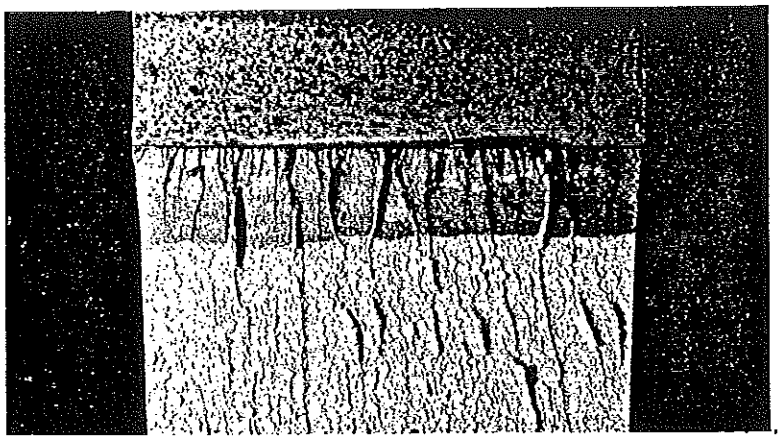

(a) MGLA 4

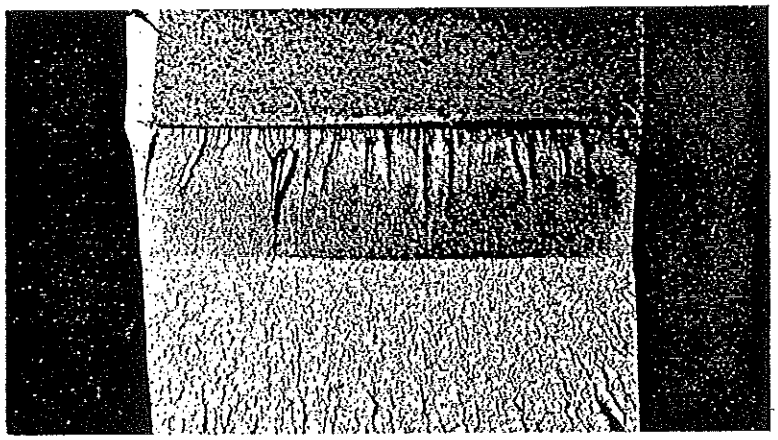

(b) MGLA 5

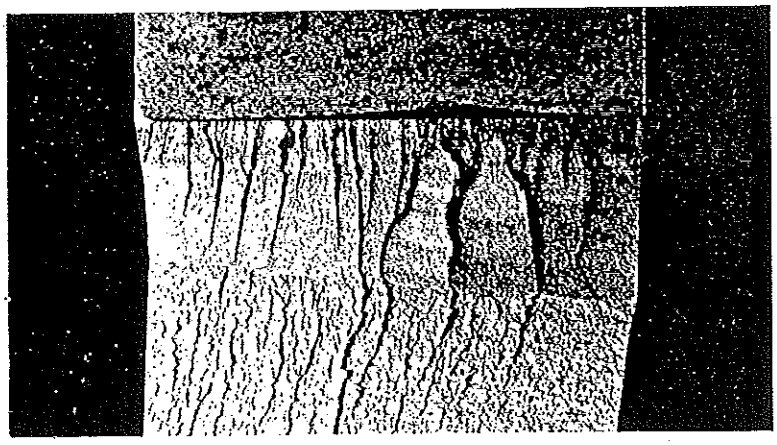

(c) MGLA 6

FIG. 4 FRACTURE SURFACES $\beta = 75^{\circ}$

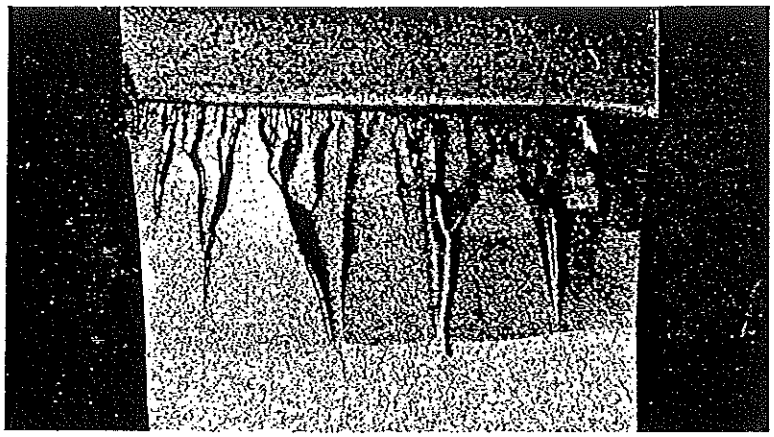

(a) MGLA 7

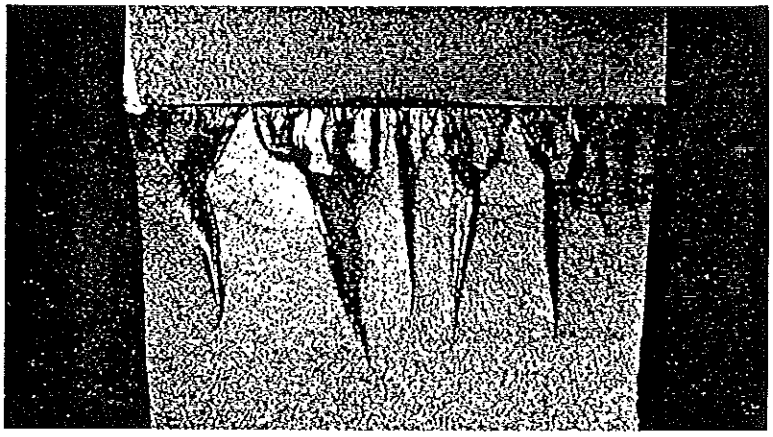

(b) MGLA 8

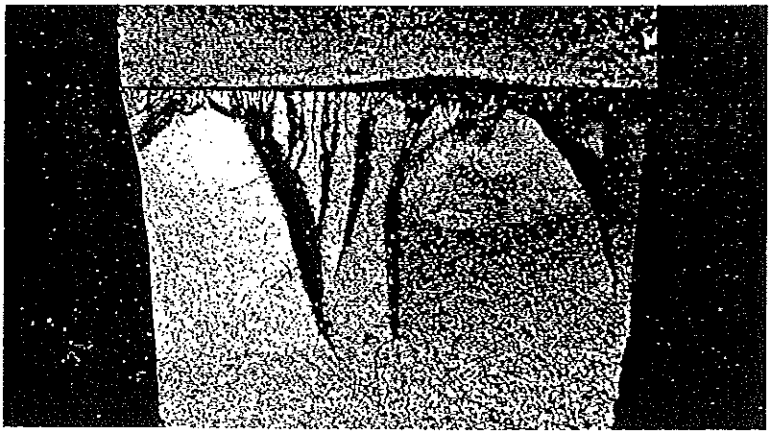

(c) MGLA 9

FIG. 5 FRACTURE SURFACES $\beta = 60^{\circ}$

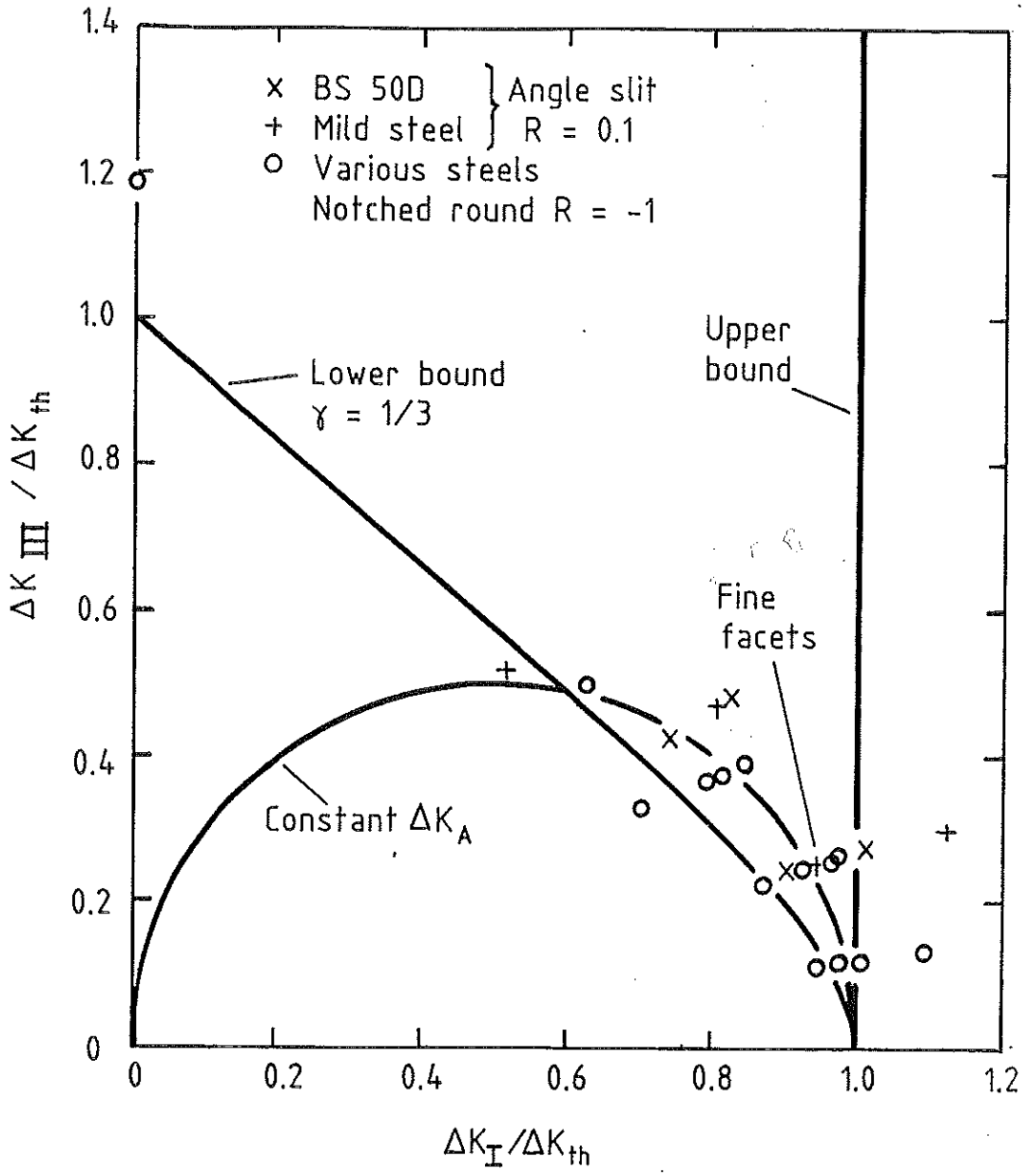

FIG. 6 FAILURE ENVELOPES FOR MIXED MODE I AND III LOADING